LASER INTERFEROMETER GRAVITATIONAL WAVE OBSERVATORY

LIGO

LIGO Laboratory / LIGO Scientific Collaboration

LIGO

Design of the Elastomeric Sealed, High Quality, Viewports

[an element of the Advanced LIGO, Auxiliary Optics Subsystem (AOS), Stray Light Control (SLC)]

Dennis Coyne

Distribution of this document:
LIGO Scientific Collaboration

This is an internal working note
of the LIGO Laboratory.

California Institute of Technology
LIGO Project – MS 18-34
1200 E. California Blvd.
Pasadena, CA 91125
Phone (626) 395-2129
Fax (626) 304-9834
E-mail: info@ligo.caltech.edu

Massachusetts Institute of Technology
LIGO Project – NW22-295
185 Albany St
Cambridge, MA 02139
Phone (617) 253-4824
Fax (617) 253-7014
E-mail: info@ligo.mit.edu

LIGO Hanford Observatory
P.O. Box 159
Richland WA 99352
Phone 509-372-8106
Fax 509-372-8137

LIGO Livingston Observatory
P.O. Box 940
Livingston, LA 70754
Phone 225-686-3100
Fax 225-686-7189

http://www.ligo.caltech.edu/

Contents

List of Figures

List of Tables

1   Introduction

The sealing process for commercial viewports often distorts the edges of the substrate. In addition, the anti-reflection (AR) coatings do not reach the edges of the optic due to shadowing effects thus reducing the clear aperture. The high quality optics required for some of the Advanced LIGO (aLIGO) viewports are most easily acquired as separate optical elements which must then be sealed for high vacuum in a viewport assembly. There are quite a number of techniques[1] that can be used for accomplishing these seals (e.g. brazing, indalloy[2], elastomers[3], etc.). We have chosen to use elastomeric seals, which allow for easy replacement and minimizes the risk of damage to the high quality optic during assembly steps.

Proper design of the viewport and the elastomeric seal must account for the fragility of the optical window and the tolerances of the components. The design criteria and the design details for high quality viewports, which are sealed to the chamber ports (via conflat seals), are considered in this memo. These viewports must sustain one atmosphere of pressure load. They are sealed to the chamber ports with a copper gasket, conflat seal.

The design of the septum plate viewports is quite similar. These viewports must sustain atmospheric pressure in either direction.

2   Design Considerations

The instances, purposes and locations for all of the aLIGO viewports, including the high quality viewports, are defined in the AOS/SLC Viewports Final Design Document[4]. Most of the ports to which the high quality viewports are attached are 10" conflat viewports. There is one instance on a 12" conflat port; The HAM2 chamber, D8 port (on top) will be used for a parking beam dump.

Some of the high quality viewports are wedged (.75 deg, [D1101005](#)) and some are not wedged ([D1101006](#)), but all are 6 in diameter optics with .75 in (minimum) thickness.

Two basic conditions must be met for reliable elastomeric window seals[3,5]:

1) The window should have no bending strain due to the clamping forces in the assembly, i.e. the force should be applied on both sides of the window at the same diameter
2) The window should not be pressed against any hard material

The design concept proposed by Roth (Ref. 5) and P.J. Abbott (Ref. 3) is shown in Figure 1. The vacuum is sealed with a compressed o-ring. A gap remains between the window and the flange. This gap is defined by the metal-to-metal contact of the window clamp and the flange, with proper consideration of the tolerances of the components and assembly. The spacer (not suggested by either Roth or Abbott, but employed in the LIGO 40m lab and suggested in Brookhaven National

---

[1] A. Roth, Vacuum Sealing Techniques, New York , American Institute of Physics, c1994

[2] S.G. Cox, P.F. Griffin, C.S. Adams, E. Riis and D. DeMille, Rev. Sci. Inst 74, 3185 (2003)

[3] P.J. Abbott, B. Scace, Safely mounting glass viewports to elastomer sealed vacuum flanges, J. Vac. Sci. Technol. A 28(4), Jul/Aug 2010

[4] M. Smith, L. Austin, Viewports Subsystem Final Design Document, LIGO-[T1000746](#)-v3, 21 Mar 2011

[5] A. Roth, Vacuum Sealing Techniques, AIP Press, 1994, section 72.8

Labs guidance[6]) is an optional element in the event that the manufactured tolerances exceed the design tolerances.

The clamping ring can be an o-ring (as suggested by Abbott), or a less compliant polymer such as PEEK.
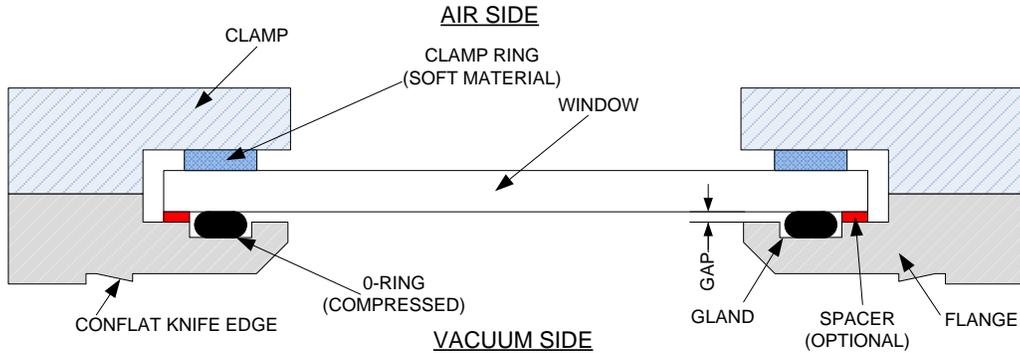
Figure 1   **Viewport with elastomeric seal (one o-ring)**

2.1 Clamp Ring or O-Ring?

Since a vacuum-tight seal is only needed on one side for the chamber viewports, one could employ a somewhat rigid (compared to an o-ring), clamping ring, comprised of a plastic, for example PEEK (as depicted in Figure 1). The clamping ring hardness would need to be much less than the window material to prevent damage to the window. This design confines all of the compression to the one o-ring. However, all of the tolerances must then be accommodated by the single o-ring (window thickness tolerance, gland depth tolerance, clamp depth tolerance and clamp ring thickness tolerance). Alternatively with o-rings on both sides (with equal compliance) only half of the total tolerance stack up must be accommodated by the compression of each o-ring.

Since the septum viewports require a vacuum seal for an atmosphere of pressure in either direction, o-rings will be employed in the design on both sides. In order to have a common design, a two o-ring approach will be used for both applications.
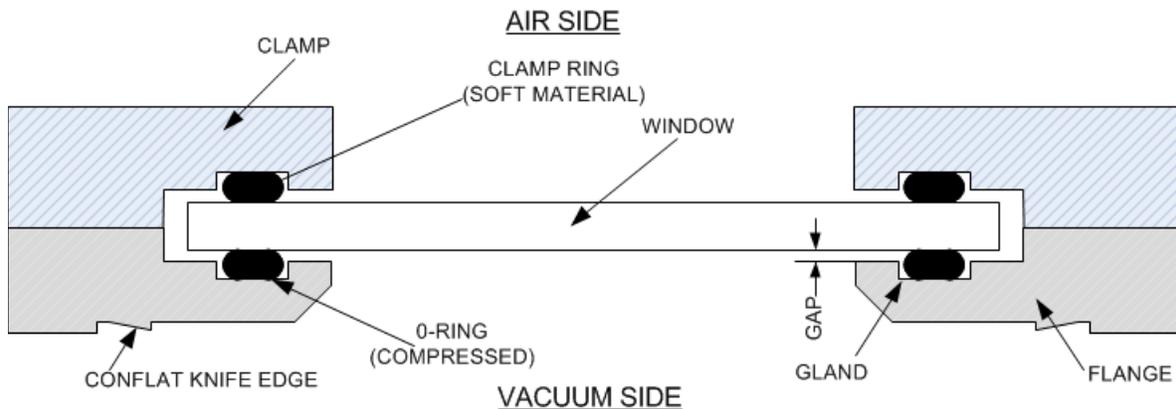
Figure 2   **Viewport with elastomeric seal (two o-rings)**

---

[6] Figure 10 of "Guide for Glass and Plastic Window Design for Pressure Vessels", Brookhaven National Labs, 2.0/17606e011.doc, 6 Nov 2008.

2.2 O-Ring Material

The most appropriate o-ring material for LIGO application is a fluoroelastomer, such as Viton™ or Fluorel™. They can be baked at moderate temperatures and have low outgassing. The most commonly available fluoroelastomer o-rings have a Shore A hardness of 75. When o-rings are purchased their specification is generally for a Shore A hardness tolerance of ±5.

2.3 Optimum O-Ring Compression

For a vacuum-tight seal, the o-ring must be compressed to an appropriate ratio of its initial height. The appropriate compression ratio range depends upon the o-ring material and the desired leak rate. Leak rate versus compression ratio is shown in Figure 2. For LIGO we only use dry (greaseless) o-rings. The implication from Figure 2 would be to design for close to 50% compression ratio. However, too much compression can cause damage to the o-ring. Appropriate values for compression ratio, as a function of hardness, are shown in Figure 3.

For a Shore A hardness of 75, the appropriate compression ratio range is between 8% and 25%. Obviously for reduced leak rate one should design for the higher end of the compression range.
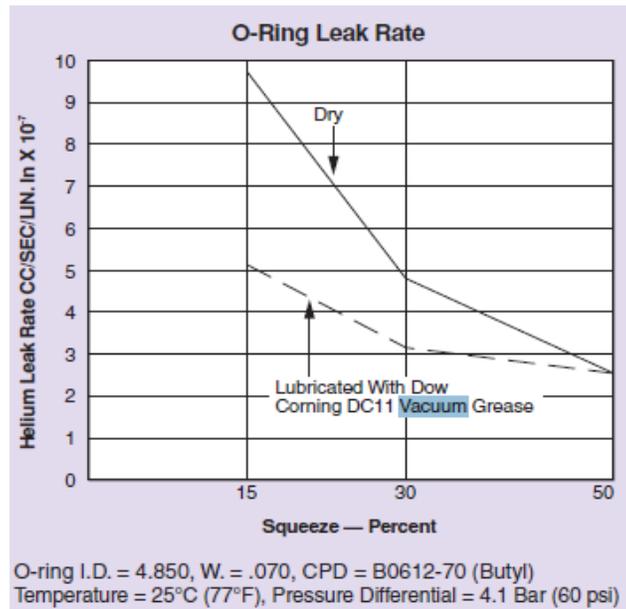
Figure 3   Leak Rate vs Compression
(Figure 3.8 of the Parker O-Ring Handbook[7])

---

[7] Parker O-Ring Handbook, ORD 5700, Parker Hannifin Corporation, O-Ring Division, copyright 2007.
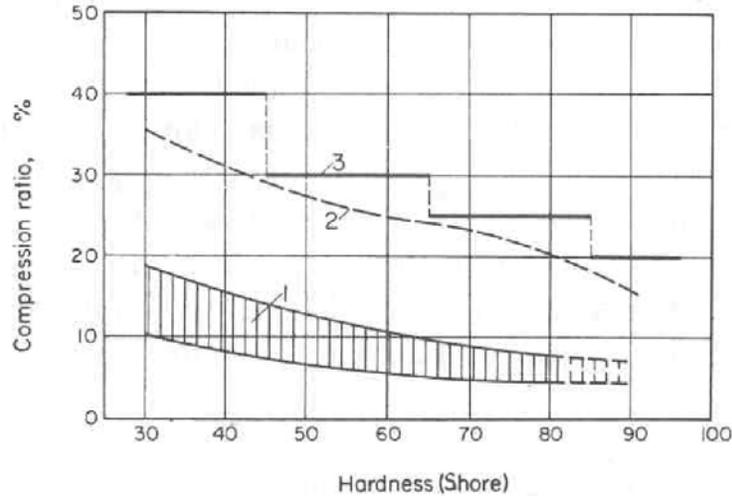
Figure 4   Compression Ratio limits for rubbers as a function of their durometer (Shore) hardness[8]. (1) minimum compression ratio needed for a vacuum-tight seal; (2) permissible compression ratio (Guthrie[9]); (3) maximum compression ratio for compression set test, ASTM 395-49T

2.4 Gap

In order to comply with the stipulation that the window not be pressed against a hard material, there must be a gap between the window and the flange, and between the window and the clamp.

2.4.1 Maximum Gap

Due to the pressure difference there is a maximum allowable gap so as not to have the o-ring extrude out of the gland. The maximum radial clearance, as a function of the pressure and o-ring hardness, is given in Figure 4. For our face seal application, the extrusion pressure should be similar to a radial seal application. In our application the pressure is 1 atmosphere (1 bar), so the maximum gap is .031 inch (conservatively).

---

[8] Figure 3.50 of A. Roth, <u>Vacuum Sealing Techniques</u>, New York , American Institute of Physics, c1994

[9] A. Guthrie and R.K. Wackerling, <u>Vacuum Equipment and Techniques</u>, McGraw Hill, New York, 1949.
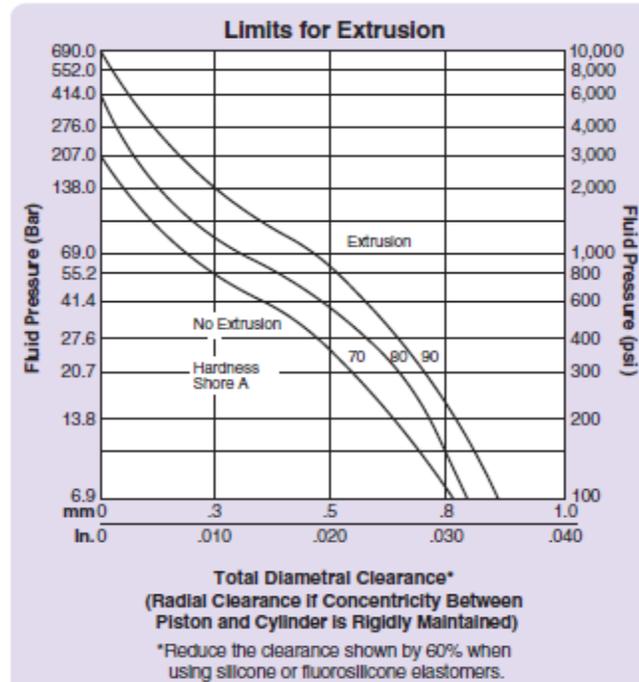
Figure 5   Maximum Allowable Clearance (Gap)
(Figure 3-2 of the Parker Handbook[7])

2.4.2 Minimum Gap

The minimum design gap must be large enough to prevent the window from contacting the metal flange or clamp when deflected under the atmospheric pressure load. A minimum gap of .005 inch should suffice (under the worst case tolerances).

2.5 Gland Design

For sealing a vacuum, the inner diameter, d_g, should be[1]:

$$d_g = D - .15d$$

where D is the o-ring inner diameter and d is the o-ring cross-sectional diameter.

The gland depth is chosen to keep the compression ratio within the allowable range given the tolerances of the flange and clamp features and the o-rings. The gland width is then set so that the fill ratio is between 60% and 90% (75% is ideal).

2.6 Window Assembly Design

The design space was first explored with the constraints given above, using an air-side, compression ring concept (instead of an o-ring), as depicted in Figure 1. At first I was trying to achieve very high compression ratios to reduce the leak rate, before I found the compression ratio limits based on o-ring hardness (section 2.3). For this scenario there was only one viable solution as indicated in Table 1.

Table 1   Summary of designs for a single o-ring and high compression ratios

#	ID	section dia.	nom	min	max	nom	min	max	nom	min	max	min	max	ID	OD	mechanical clear aperture	comment
	o-ring		compression			gland fill			clearance			air leak rate (torr-liter/sec)		Gland			
Ideal			50%			75%												for high vacuum HOWEVER this exceeds the maximum compression for 75 Shore A hardness
Criteria			≥ 20%			≥ 60%	≤90%		≥ .005	≤ ~.031					≤ 5.895	≥ 5.200	
#2-252	5.23											1.4E-06	2.5E-06	5.234		5.134	mech clear aperture < optical clear aperture
#2-253	5.359	0.139	29%	20%	39%	74%	61%	90%				1.4E-06	2.6E-06	5.338	5.804	5.238	The only solution which meets all criteria
#2-254	5.484											1.5E-06	3.0E-06	5.484	5.904	5.384	gland OD too close to optic edge
#2-355	5.225											1.4E-06	2.2E-06	5.225	5.855	5.125	mech clear aperture < optical clear aperture
#2-356	5.350	0.210	33%	27%	39%	78%	68%	90%	0.018	0.005	0.031	1.5E-06	2.2E-06	5.350	5.980	5.250	gland OD exceeds optic face OD
#2-357	5.475											1.5E-06	2.3E-06	5.475	6.105	5.375	gland OD exceeds optic face OD
#2-431	5.225											1.3E-06	1.7E-06	5.225		5.125	mech clear aperture < optical clear aperture
#2-432	5.350	0.275	38%	33%	43%	79%	71%	90%				1.3E-06	1.7E-06	5.350	6.230	5.250	
#2-433	5.475											1.4E-06	1.8E-06	5.475	6.355	5.375	gland OD exceeds optic face OD
0) All dimensions in inches																	
1) All critical dimensions toleranced at ± .001 in																	
2) Trading mechanical aperture for leak rate: An air leak rate of 2.9e-6 vs 1.7 t-l/s results in an increase of 1 nTorr in the vertex/diagonal sections or 2 nTorr in the end stations. Compare to a pressure of 20 nTorr in these volumes (10 nTorr in the LLO end stations). This is a weak function																	

Realizing that it would be best to have a common design for both the external viewports, as well as the internal, septum plate viewports, I then converted the compression ring to an o-ring with identical dimensions as the sealing o-ring. If the two o-rings are identical, then their spring rates are equal ("balanced") and the effect of the tolerance stack up in the design allows:

- a variation in compression from 18% to 27% (slightly above the recommended maximum for 75 Shore A hardness)
- a variation in gap from .014 in to .026 in

as shown in Table 2.

Also shown in Table 2 is the case where the o-rings have the same Shore A hardness, but the compression spring rates are at the minimum and maximum indicated in Figure 12. In this case either the compression ratio is too high or the gap is too little or too large. Therefore it is important that the o-ring pair used in an assembly come from the same batch or lot to insure nearly identical behavior. I have been assured by a Parker representative that o-rings from the same batch/lot will have identical Shore A hardness and should match closely in the compression force required to achieve a given compression ratio. See also section 4.3.

Table 2   Effect of tolerances for the two o-ring design

Balanced o-rings:			Min/Max o-rings:			
nominal	min tol	max tol	nominal	min tol	max tol	
0.108	0.102	0.114	0.096	0.087	0.104	B1, compressed height of o-ring1
0.108	0.102	0.114	0.120	0.117	0.124	B2, compressed height of o-ring2
0.223	0.266	0.180	0.313	0.371	0.255	c1, compression on o-ring1
0.223	0.266	0.180	0.133	0.162	0.105	c2, compression on o-ring2
9.083	13.283	5.675	18.721	26.743	12.120	F1, force per unit length of o-ring1 (min 70 Shore A)
9.083	13.283	5.675	18.721	26.743	12.120	F2, force per unit length of o-ring2 (max 70 Shore A)
0.000	0.000	0.000	0.000	0.000	0.000	F2-F1, force balance error
0.020	0.014	0.026	0.008	-0.001	0.016	s1, gap for o-ring1
0.020	0.014	0.026	0.032	0.029	0.036	s2, gap for o-ring2

The design drawings are:

- LIGO-D1100999-v1: aLIGO, high quality, non-wedged, 6" Viewport Assembly
- LIGO-D1101000-v1: aLIGO, high quality, .75 deg wedged, 6" Viewport Assembly
- LIGO-D1101001-v1: aLIGO, high quality, 6" Viewport Flange
- LIGO-D1101002-v1: aLIGO, high quality, 6" Viewport Clamp
- LIGO-D1101115-v1: aLIGO, high quality, 6in Viewport Clamp, wedged
- LIGO-D1101092-v1: aLIGO Septum Viewport Assembly
- LIGO-D1101117-v1: aLIGO, Septum Viewport Flange

3 Leak Rate

The leak rate of a gas through an O-ring seal may be calculated with the following approximate formula[10]:

$$L = 0.7 \, F \, D \, P \, Q \, (1-S)^2$$

where

L = Approximate leak rate of the seal, std. cc/sec.

F = Permeability rate of the gas through the elastomer at the anticipated operating temperature, std. cc cm/cm² sec bar

D = Inside diameter of the O-ring, inches.

P = Pressure differential across the seal, lb/in²

Q = Factor depending on the percent squeeze and whether the O-ring is lubricated or dry (Figure 6)

S = Percent squeeze (compression) on the O-ring cross section expressed as a decimal. (i.e., for a 20% squeeze, S = .20)

This formula gives only a rough order of magnitude approximation because permeability varies between compounds in the same polymer, and because the assumptions on which it is based are not all exact.

---

[10] Sections 3.11.3 and 3.12.1 of the Parker O-Ring Handbook, ORD 5700, Parker Hannifin Corporation, O-Ring Division, copyright 2007

Effect of Squeeze and Lubricant on O-ring Leak Rate

For helium leak rate, a variation of ±50% from the predicted value should be anticipated to allow for limitations in the accuracy of test equipment and available standards, and for variations between samples.
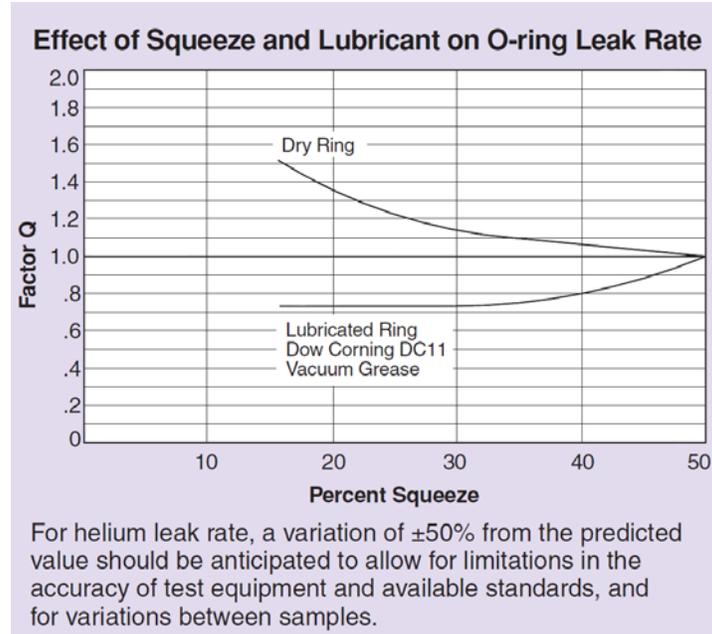
Figure 6   Factor Q for leak rate calculation

The Parker Handbook[7] does not give the permeability of air through a fluoroelastomer. However this can be estimated by the permeability of the two primary gases which compose air, ~80% N_2 and ~20% O_2:

$$F_{air} = (.8 \text{ x } .233 + .2 \text{ x } .17) \text{ x } 10^{-8} = 5.3 \text{ x } 10^{-9} \text{ std. cc cm/cm}^2 \text{ sec bar}$$

With a nominal 20% compression, Q = 1.35. For a #2-253 o-ring with an inner diameter D = 5.359 in and

$$L_{air} = 2.5 \text{ x } 10^{-7} \text{ std. cc/sec} = 1.9 \text{ x } 10^{-7} \text{ torr-liter/sec}$$

For He, $F_{HE} = 12.8 \text{ x } 10^{-8}$ std. cc cm/cm^2 sec bar and

$$L_{He} = 6.1 \text{ x } 10^{-6} \text{ std. cc/sec} = 4.6 \text{ x } 10^{-6} \text{ torr-liter/sec}$$

As a sanity check, compare this air leak rate to a value of 10^{-5} torr-liter/sec for a 60.5 inch diameter o-ring, as calculated by PSI for the LIGO large seals[11]. Scaling to these 6 inch diameter windows gives a leak rate of 10^{-6} torr-liter/sec, about a factor of 5 larger than calculated above, but within an order of magnitude.

The effect of this leak rate on the overall pressure in each of the LIGO vacuum volumes, given the number of viewports to be installed, is calculated[12] to be ~0.3 nTorr.

4   Stress Analysis

A stress analysis is only needed for the window due to its fragility. The o-ring will, by design, only be compressed within allowable limits. The response of the window is both materially linear (linear

---

[11] PSI V049-1-097, Rev.0, section 3.3.5

[12] Using the spreadsheet associated with: M. Zucker, D. Coyne, Advanced LIGO residual gas estimate, LIGO-E0900398-v6

elastic material) and geometrically linear (small displacement). The response of the fused silica material is well approximated by a linear elastic, isotropic constitutive equation. The elastic (Young's) modulus[13] for the fused silica window material is E = 73.6 GPa and the Poisson's ratio is ν = 0.17.

The exact distribution of the compression stress on the window depends on the details of the compression of the o-ring. In order to precisely calculate the o-ring deformation one would need to perform a nonlinear analysis accounting for the nonlinear, viscoelastic material response of the fluorocarbon material and accounting for the large displacement/deformation response of the o-ring. However, a reasonable approximation can be made by simply assuming a uniform pressure at the interface of the o-ring with the window. The width of this annular contact region can be estimated by assuming that the cross-section of the o-ring is as shown in Figure 7. Since the o-ring response is essentially incompressible, the annular width, L, is:

$$L = \frac{\pi(d^2 - H^2)}{4H}$$

where d is the o-ring uncompressed cross-sectional diameter and H is the compressed height of the o-ring. The squeeze fraction is H/d and the compression ratio is 1-H/d.
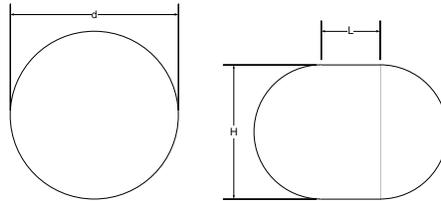
Figure 7   Compressed o-ring profile

4.1 Allowable stress for Fused Silica

It is well established that subcritical crack growth in glasses and ceramics, in environments containing water vapor, is caused by a tensile stress enhanced, chemical corrosion at the tip of pre-existing surface flaws[14]. This phenomenon is known as "delayed failure" or "static fatigue".

Weiderhorn et. al. found that some glasses exhibited subcritical crack growth in vacuum, whereas some other glasses did not (including two that had anomalous elastic behavior and an Ultra-Low Expansion (ULE) glass). I am unaware of any studies on subcritical crack growth for fused silica in vacuum. It is possible (even likely) that fused silica does not exhibit subcritical crack growth (static fatigue) while under vacuum. However, it is important to consider the lifetime and strength due to static fatigue in this application, because (a) the viewports are cycled up to air multiple times and

---

[13] One might be tempted to think that the bulk modulus, K, of the window material is the most relevant elastic property since it is a measure of the material's resistance to a uniform pressure and the primary load on the window is pressure. However, this pressure is not uniform and the principal response of the window is in bending, not uniform compressive dilatation. Moreover the constitutive equations employed in the finite element formulation define the bulk modulus as

$$K = \frac{E}{3(1 - 2\nu)}.$$

[14] K. Jakus, D. Coyne, J. Ritter, Analysis of fatigue data for lifetime predictions for ceramic materials, J. Materials Science, 13 (1978) 2071-2080.

for significant durations during its lifetime and (b) there can be tensile stresses on the air side of the viewport windows (as explained in following sections).

Pre-existing flaws grow in size under the service load (stress) to a critical size at which a crack propagates quickly. The subcritical growth can be expressed as a power function of the stress intensity factor, K_I:

$$V = AK_I^N$$

where V is the crack velocity, A and N are constants that depend on the environment and material composition. From this equation it can be derived that the time to failure, t_f, under a constant tensile stress, σ_a, is:

$$t_f = BS_i^{N-2}\sigma_a^{-N}$$

where $B = 2/(AY^2(N-2)K_{IC}^{N-2})$, Y is a geometric constant ($\sqrt{\pi}$ for surface flaws), K_{IC} is the critical stress intensity factor and S_i is the fracture strength in an inert environment.

The probability distribution function for the inherent fracture strength is often well modeled by a Weibull function:

$$\ln\left(\ln(\frac{1}{1-F})\right) = m\ln\left(\frac{S_i}{S_0}\right)$$

where F is the cumulative failure probability and m, S_0 are constants.

There does not seem to be much data on subcritical crack growth for fused silica in the literature[15], other than for fused silica fibers. While the crack propagation parameters are expected to be material constants (and so fused silica fiber properties would be applicable to fused silica in 'plate' form), the strength distribution parameters would be markedly different. However there is a NIST study[16] on two Corning grades of fused silica which has subcritical crack growth parameters based on macroscopic crack growth measurements, as well as static and dynamic fatigue testing. The results of these three measurement sets were consistent, although there was considerable uncertainty in the parameters due to the limited sample size. The subcritical crack growth parameters from this study are summarized in Table 1. Other published data for fused silica fibers have N values of 36 < N < 44 (reference[17]) and 19 to 21 (reference[18]). The significant differences between the values from the various data sets likely reflect the relatively small sample size (order of 40 samples in each set). However, in addition microscopic flaws likely propagate quite

---

[15] Although my search in the literature cannot be claimed to be exhaustive.

[16] L. Braun, J. Wallace, E. Fuller Jr., "Fracture Mechanics and Mechanical Reliability Study Comparison of Corning Code 7980 and Code 7940 Fused Silica", National Institute of Standards and Technology, Final Report to NASA, Nov 1998 (draft)

[17] M. Muraoka, A. Hiroyuki, "Subcritical crack growth in silica optical fibers in a wide range of crack velocities", J. Am. Ceram. Soc., 79 [1] 51-57 (1996).

[18] B.A. Proctor, I. Whitney, J.W. Johnson, "Strength of Fused Silica", Proc. R. Soc. London, Ser. A, 297 [1451] 534-57 (1967). As reported in reference 19

differently than large, pre-formed cracks in samples[19]. For reasons discussed in the source document, the parameters derived from the dynamic fatigue data set have higher confidence than for the static fatigue data set.

Table 3   Subcritical crack growth parameters for fused silica

N.B.: In the dynamic fatigue data set, samples which had visible tensile surface scratches were excluded from the analysis. However, when samples with visible tensile surface defects were excluded from the static fatigue data set, unrealistically high values of N resulted, so these samples were kept in the analysis.

Data Set	N	B (MPa^2 s)	m	S$_0$ (MPa)
Corning 7980 Macroscopic crack velocity data	38.4			
Corning 7940 Macroscopic crack velocity data	38.7			
Corning 7980 Dynamic fatigue data	40.5	5.1 x 10^{-4}	4.4	156.5
Corning 7980 Static fatigue data	31.1	8.6 x 10^{-6}	4.4	156.6

A plot of the allowable tensile stress as a function of cumulative failure probability and desired lifetime is shown in Figure 7, for the parameter set based upon the dynamic fatigue data. For a desired lifetime, t_f, of 20 years (6.31 x 10^8 sec) and a tolerable cumulative failure probability F = 10^{-5}, <u>the allowable applied stress, σ_a, is 5.1 MPa (740 psi); This will be taken as the tensile limit stress in service.</u> The corresponding inert strength, S_i, is 11.4 MPa (1659 psi).

The allowable (or design, or working) tensile stress is the tensile limit stress divided by the required (or design) Factor of Safety (FS); see section 4.5.

As a sanity check, these values (σ_a and S_i) compare well to:

   a) the tensile limit load (allowable tensile stress at limit load) of 800 psi and presumed ultimate tensile stress value of 1600 psi which were used in a NASA project[20] for fused silica.
   b) the allowable design stress of 680 psi given in the Brookhaven National Labs guidance for fused silica[21]

---

[19] J.E. Ritter, K. Jakus, "Applicability of Crack Velocity Data to Lifetime Predictions for Fused Silica Fibers", J. Am. Ceram. Soc., Mar-Apr 1977, 171.

[20] C. Sheppard (Talandic Research Corp.), "Allowable stresses for BK7 and fusd silica components used in WCE equipment", letter to M. Yokely (Kaman Sciences Corp.), 20 Nov 1987. Based on design stress values given by Schott Corp.

[21] Table 1 of "Guide for Glass and Plastic Window Design for Pressure Vessels", Brookhaven National Labs, 2.0/17606e011.doc, 6 Nov 2008, which is based on data extracted from Corning Code No. 7940 "Fused Silica". However this allowable design stress value was arrived at by simply stipulating a Factor of Safety of 10 to use with an ultimate strength of 6,800 psi (46.9 MPa)

Contrast these values to the ultimate strength value of 50 MPa for fused silica reported in Yoder[22]. This corresponds to a cumulative failure probability F = 0.5 and a time to failure, tf = 0, i.e. the average instantaneous failure strength.
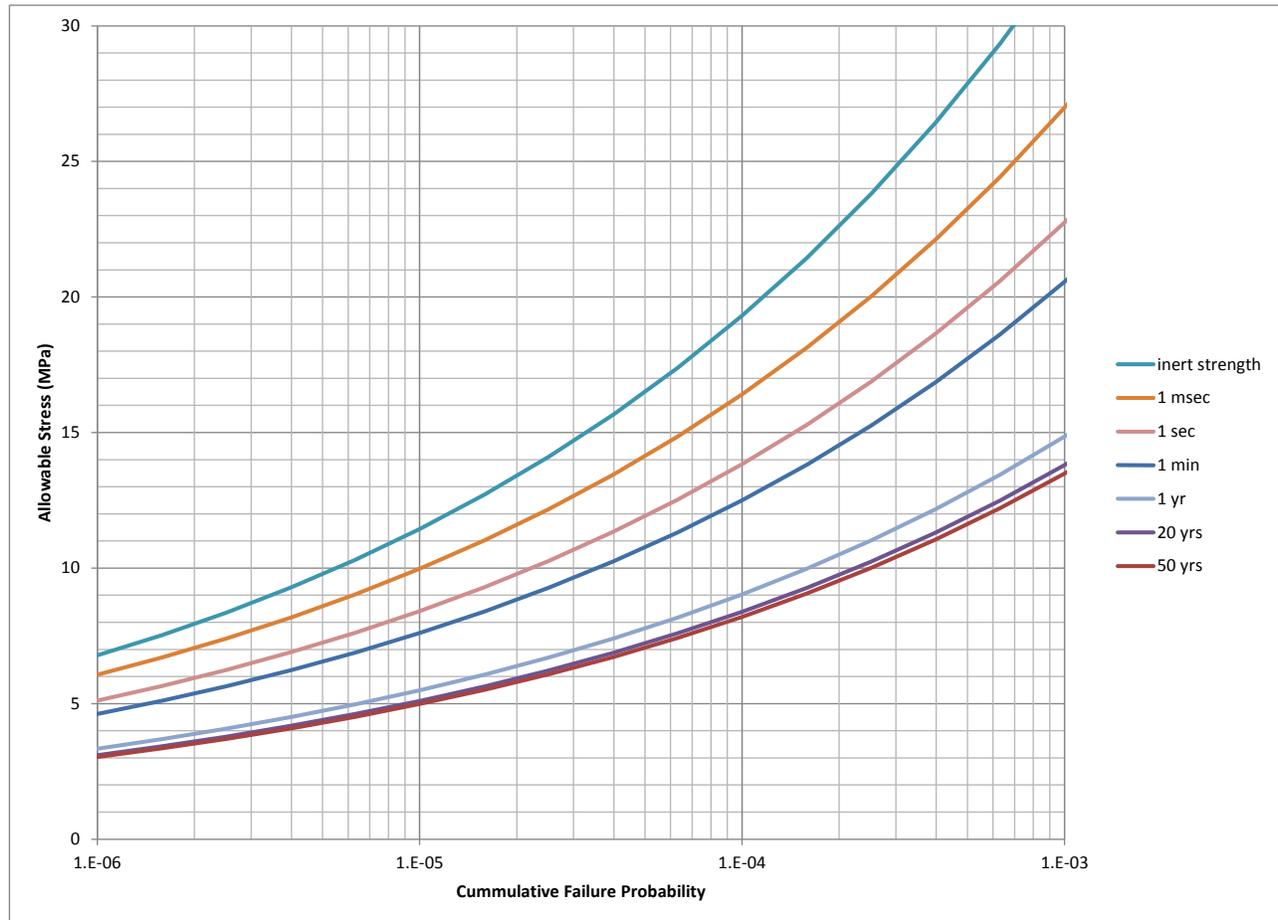
Figure 8   **Allowable stress versus cumulative failure probability**

4.2 Stress due to the Pressure Load

The response (deflection and stress) of the window/optic due to one atmosphere of load can be estimated by the response of a circular flat plate of constant thickness loaded with a uniform pressure on one side and simply supported at its perimeter[23]:

$$y_c = \frac{-qa^4(5+\nu)}{64D(1+\nu)}$$, the deflection of the plate (window) at the center

$$\sigma_c = \frac{3qa^2(3+\nu)}{8t^2}$$, the stress at the face of the plate (window) at the center

where

---

[22] Yoder, <u>Optomechanical Systems Design</u>, Table 3.5

[23] W.C. Young, <u>Roark's Formulas for Stress & Strain</u>, 6th ed., Mc-Graw-Hill, 1989, Table 24, case 10a with $r_0=0$

16

a = radius to the simple support (taken as the compressed o-ring I.D.)

q = applied pressure load

t = window thickness

$D = \dfrac{Et^3}{12(1-\nu^2)}$ is the "plate constant", or stiffness

E = modulus of elasticity

ν = Poisson's ratio

For fused silica, E = 10.7 10^6 psi (73.6 GPa) and ν = 0.17. The calculated window center deflection and stress with a = 2.736 in, q = 14.7 psi, and t = .75 in, is shown in Table 1.

Table 4   Comparison of circular plate bending under deflection and Finite Element Analysis (FEA)

Parameter	uniform thickness, circular plate under uniform pressure load with simple support	FEA
Center deflection, y_c	-.00015 in	-.00016 in
Center, face stress, σ_c	232 psi	213 psi

A finite element analysis was performed to check the approximate formulation above. The model applied pressure (14.7 psi) over the air side of the window, as well as the sides and the lower surface which is outside of the o-ring (as shown in Figure 8). The o-ring was approximated as a compression-only support. The results are shown in the figures below and in Table 2. The approximate calculation is reasonably close to the finite element result, indicating that the response is primarily plate-like bending[24].

---

[24] Even though the window is quite thick, its response is dominated by the plate stiffness, D (i.e. the elastic modulus, E, and Poisson's ratio, ν), as opposed to the bulk modulus, K.
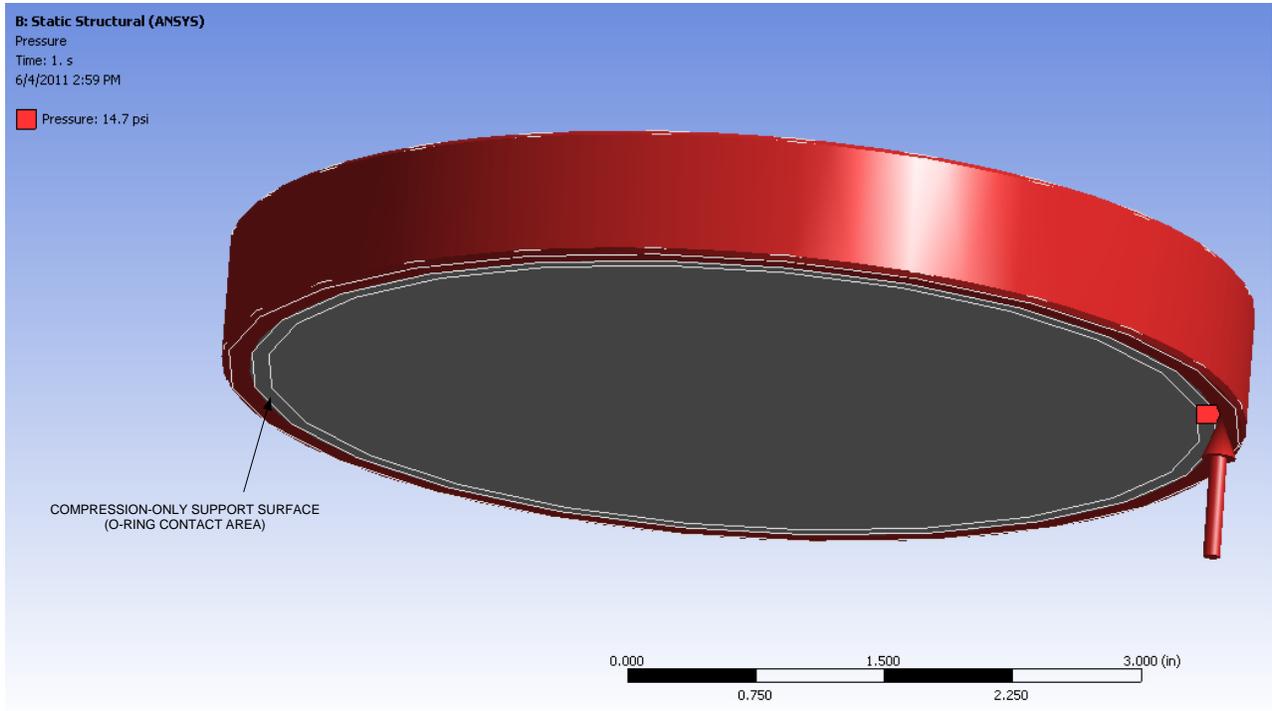
Figure 9   Boundary conditions for static pressure response calculation
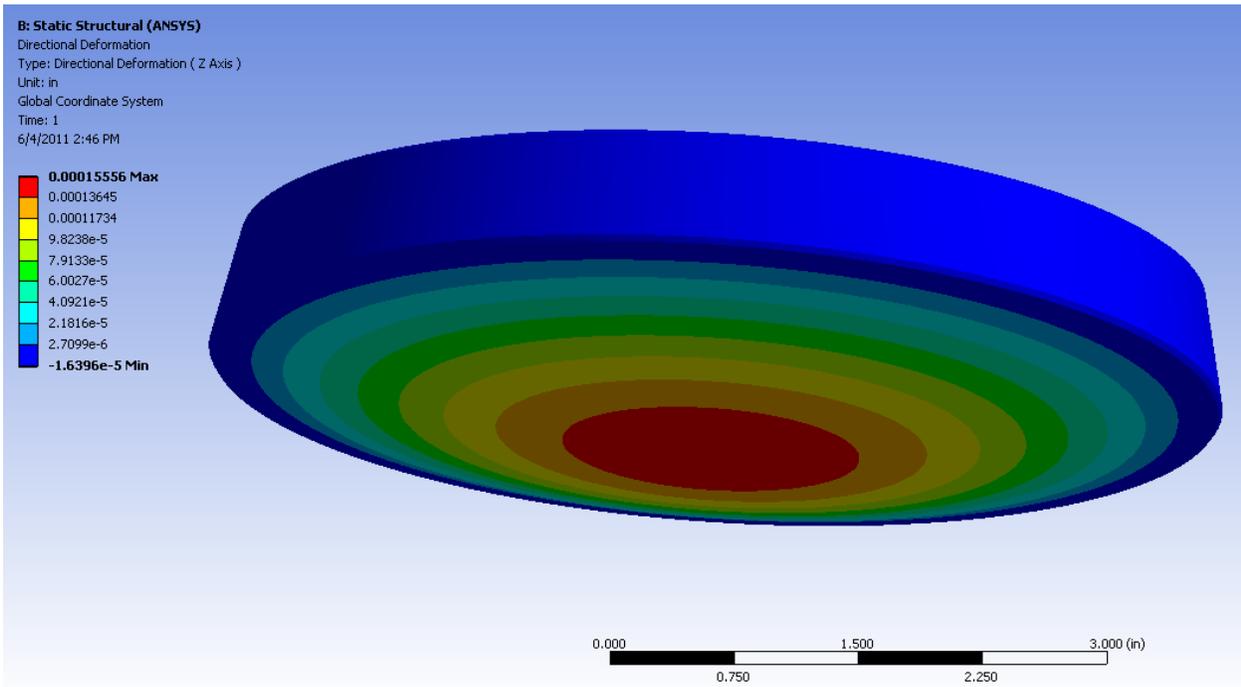
Figure 10   Axial deformation due to one atmosphere (14.7 psi). The peak deflection is .00016 in.
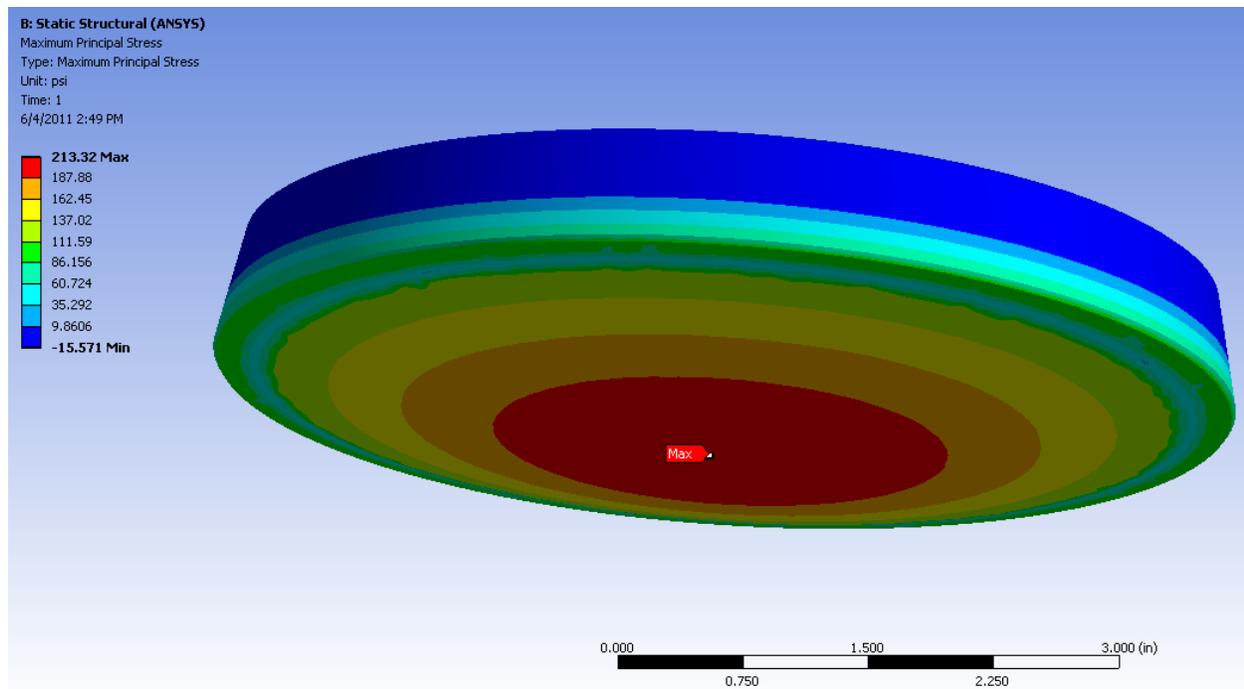
Figure 11   Maximum principal stress due to one atmosphere (14.7 psi). The peak tensile stress is 213 psi (at the center of the window on the vacuum face).

4.3 O-Ring Clamping Force

The compression force per unit length required to achieve a specific compression ratio, as a function of Shore A hardness is provided in graphs for each cross-section diameter in the Parker O-Ring Handbook[7], such as the one shown in Figure 5. For the LIGO design (#2-253 o-ring, .139 inch diameter, 75 ± 5 Shore A hardness, 10% to 25% compression range) the range of clamping force is between 2 and 71 lbf/in (by polynomial interpolation). This corresponds to a total force variation of 35 lbf to 1229 lbf, or a clamping pressure of ~20 to ~700 psi.

If a 50% compression were permitted, the maximum o-ring force would be 287 lbf/in, 4961 lbf or 2863 psi.

With the typical Shore A tolerance of ± 5, o-rings which have a nominal hardness of 75 Shore A, could require clamping forces which vary by a factor of 10! (minimum force for 70 and maximum for 80 from Figure 5). While this may be true for randomly purchased o-rings from different batches/lots, I have been assured by a Parker representative that o-rings from the same batch/lot will have identical Shore A hardness and should match closely in the compression force required to achieve a given compression ratio. This is important, otherwise most of the compression will occur in only one o-ring (which may not be the one on the vacuum side). The o-ring pairs must come from the same batch/lot.
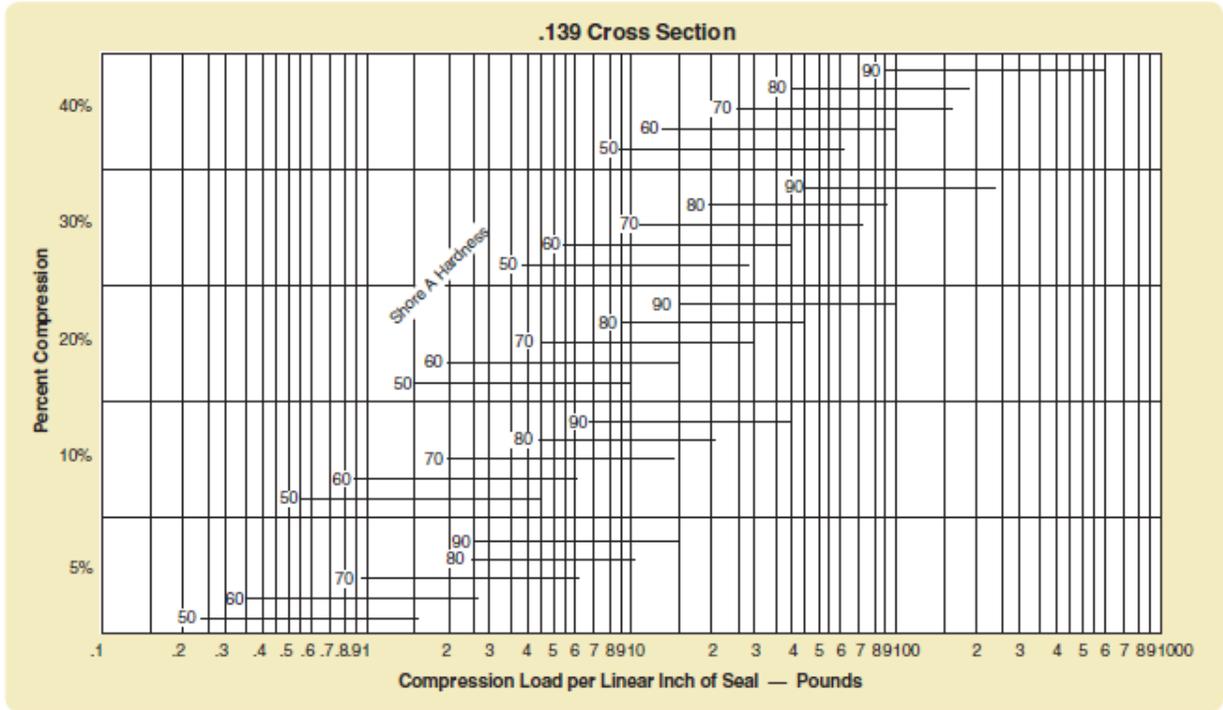
Figure 12   O-Ring Clamping Force
(Figure 2-6 of the Parker O-Ring Handbook[7])

4.4 Stress due to the Clamping Load

If the clamping ring on the air side of the window has an O.D. equal to the window, for ease in aligning in when assembling, then its radial extent does not match the o-ring on the vacuum side and the opposing clamp forces on the window create a moment (see Figure 11). The magnitude of this radial offset is only .069 in., but it is significant.

The response of the window to the moment created by the clamping forces can be approximated by the response of a simply supported, flat circular plate of constant thickness, with a uniform annular line load[25]:

$$y_c = \frac{-wa^3}{2D}\left(\frac{L_9}{1+v} - 2L_3\right), \text{ the deflection of the plate (window) at the center}$$

$$\sigma_c = \frac{6waL_9}{t^2}, \text{ the stress at the face of the plate (window) at the center}$$

where

a = radius to center of outer support (clamping ring)
w = force per unit of circumferential length

---

[25] W.C. Young, <u>Roark's Formulas for Stress & Strain</u>, 6th ed., Mc-Graw-Hill, 1989, Table 24, case 9a

$$L_3 = \frac{r_0}{4a}\left[\left(\left(\frac{r_0}{a}\right)^2 + 1\right)\ln\left(\frac{a}{r_0}\right) + \left(\frac{r_0}{a}\right)^2 - 1\right], \text{ a loading constant}$$

$$L_9 = \frac{r_0}{a}\left[\frac{1+v}{2}\ln\left(\frac{a}{r_0}\right) + \frac{1-v}{4}\left(1 - \left(\frac{r_0}{a}\right)^2\right)\right], \text{ a loading constant}$$

r0 = the radial position of the annular load (center of the o-ring)

The calculated window center deflection and stress with a = 2.855 in, r_0 = 2.7855 in, and w = 287 lb/in, is shown in Table 3.

Table 5   Comparison of circular plate bending under clamping moment and Finite Element Analysis (FEA)

Parameter	uniform thickness, circular plate under uniform annular line load with simple support	FEA
Center deflection, y_c	-.00017 in	-.00010 in
Center, face stress, σ_c	208 psi	186 psi

A finite element analysis was performed to check the approximate formulation above. The model applied pressure a uniform pressure of 1152 psi over the contact area of the clamping ring (corresponding to 287 lb/in). The contact area of the compressed o-ring was defined as a compression-only support. The results are shown in the figures below and in Table 3. The approximate calculation of the stress in the center of the window is reasonably close to the finite element result, indicating that the response in the center of the plate is primarily plate-like bending due to the moment applied by the clamp. However the deflection is not very close to the calculation for a uniform plate since the localized deflection due to the clamping force is large compared to the deflection due to bending.

Of more concern is the fact that the peak tensile stress in the window appears to be in an annular region on the o-ring sealed face of the window, just outside the o-ring (in air). At this location there is a steep gradient of stress which reaches a maximum of ~1000 psi, as shown in Figure 14. In addition there is an annular region on the window face which contacts the clamping ring, just inside the ring, where the peak tensile stress is 626 psi. This region is in air and is also more prone to contact and scratches due to (inadvertent) handling or contact.
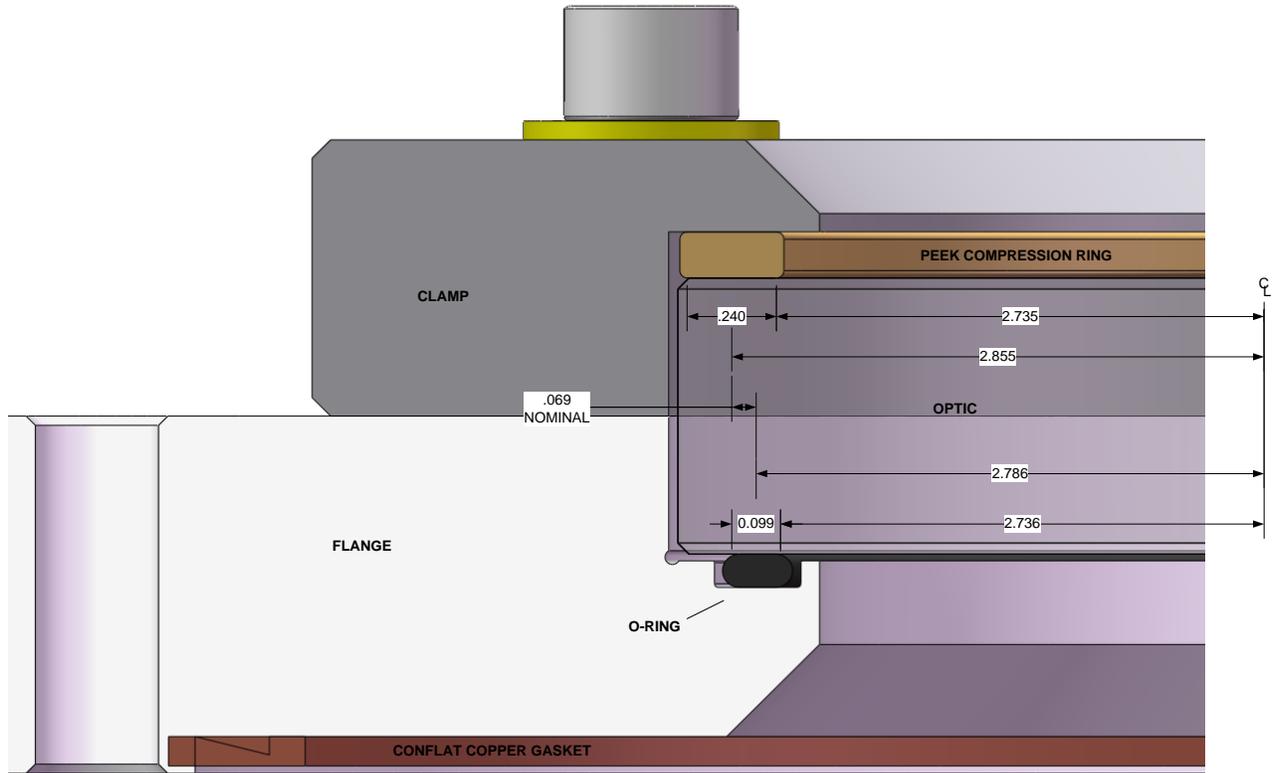
Figure 13 **Cross-section of non-wedged viewport with a radial offset between clamping ring and o-ring resulting in an applied moment due to the clamping forces**
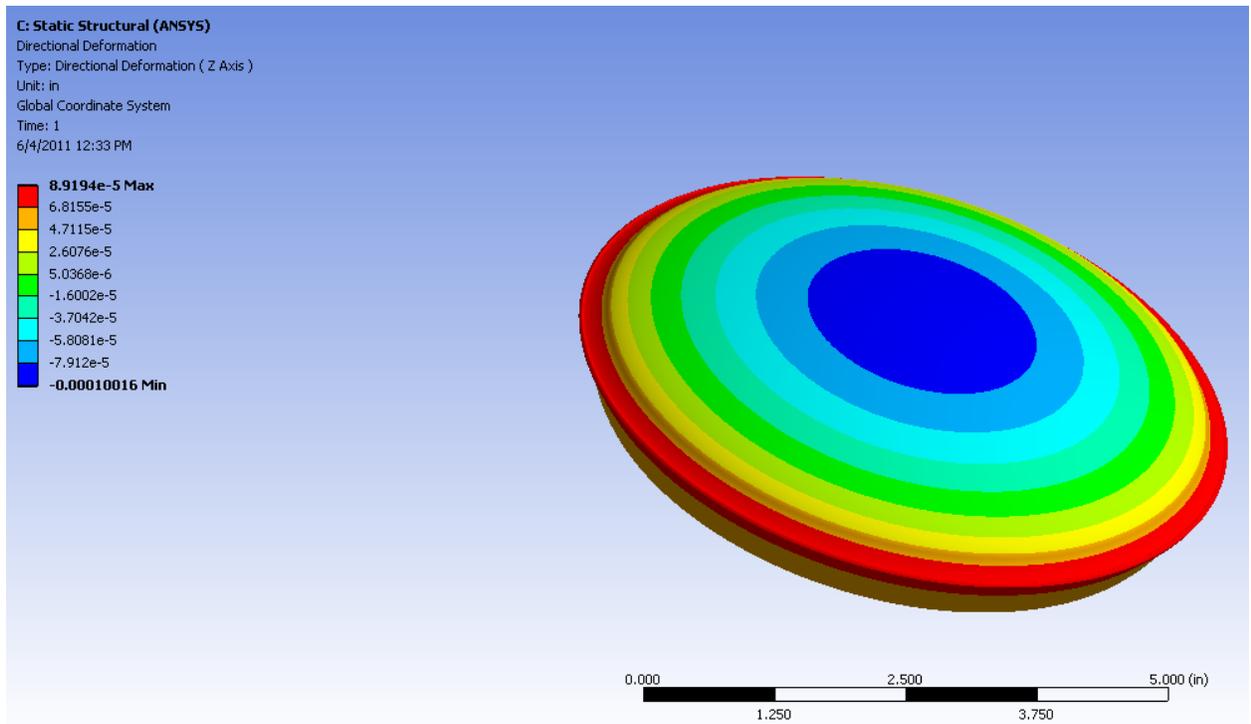
Figure 14 **Axial deformation due to clamping force & moment (.00010 " maximum)**
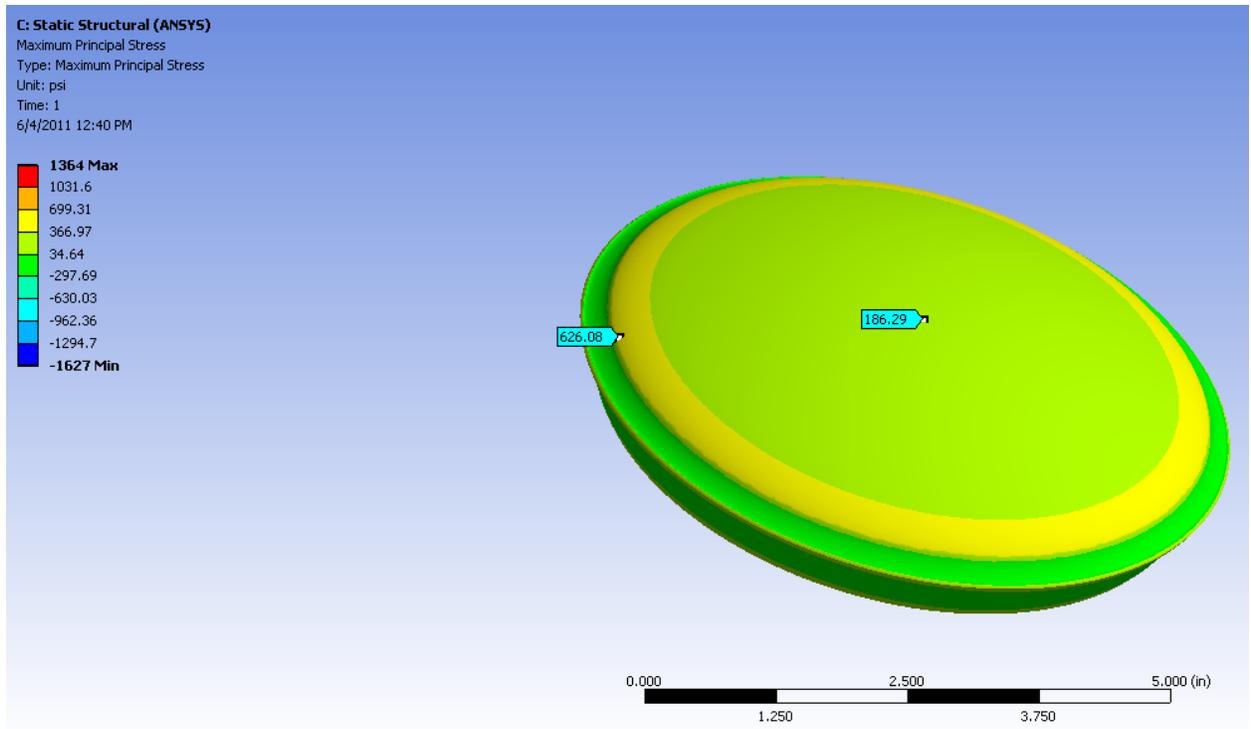
Figure 15 **Maximum principal stress on the upper (air) side, due to clamping force & moment. Maximum principal tensile stress is 626 psi. Tensile stress at the center of the plate is 186 psi.**
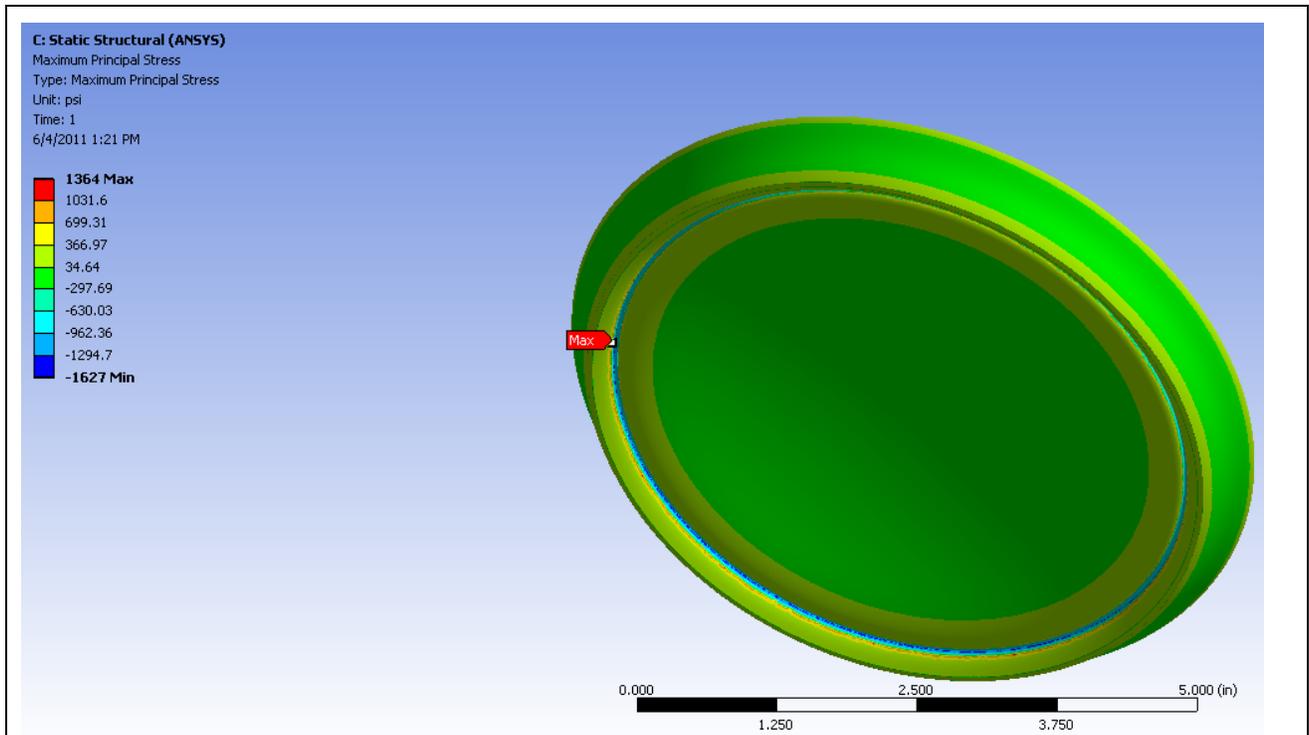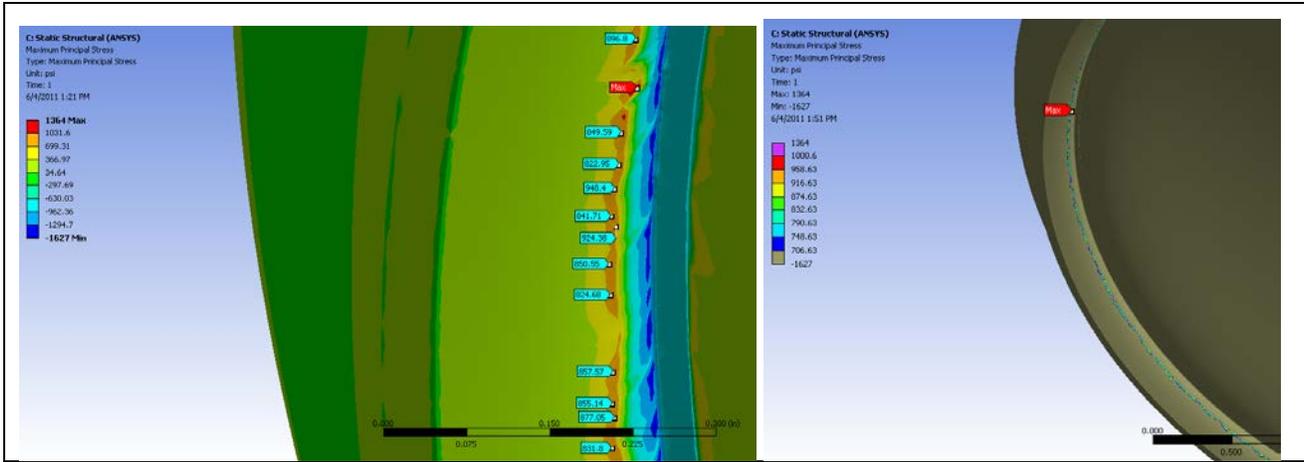
Figure 16   Maximum principal stress on the lower side due to clamping force & moment. Maximum principal tensile stress is ~1000 psi (The 1364 psi max result is a localized artifact of the finite element mesh. The mesh consisted of 1,755,237 ANSYS SOLID187 elements and 2,502,458 nodes.)

This is rather puzzling, since an analytical solution for a similar situation predicts zero principal stresses on the surface. Consider a uniformly distributed pressure (q) applied in the direction normal to a part (width 2b) of the boundary of a semi-infinite elastic medium, as depicted in Figure 16. This situation differs from the o-ring compression on the surface of the window in that:

   a) the o-ring loading is axisymmetric, not rectilinear. However, the radius of the o-ring is large compared to the dimensions of the o-ring cross-section and localized stress response, so that the stresses should be similar
   b) the window is, of course, not semi-infinite in extent. However the thickness is large compared to the dimensions of the o-ring cross-section and localized stress response, so that the stresses should be similar

(a) Principal stress trajectories are confocal hyperbolas and confocal ellipses

(b) Isochromatics are circles centered on OX_3 and passing through O_1 and O_2
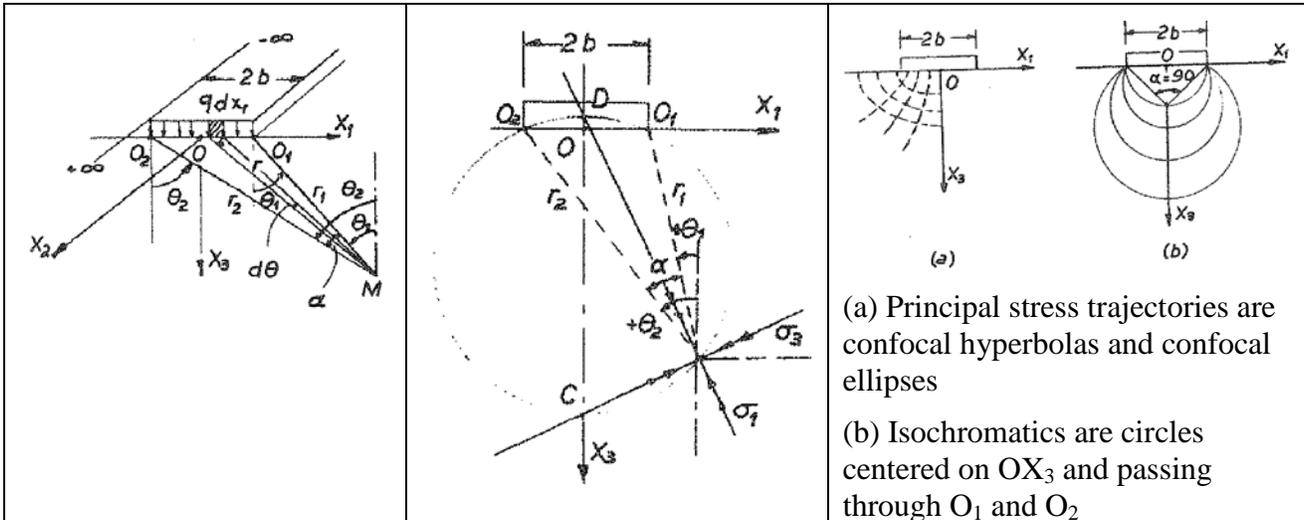
Figure 17   Uniformly distributed pressure on a part of the boundary of a semi-infinite elastic medium
(figures 14.13, 14.14 and 14.15 of Ref. 26)

24

The principal stress solution to this plane strain problem, at point M, is given by[26]:

$$\sigma_1 = -\frac{q}{\pi}[\alpha + \sin\alpha]$$

$$\sigma_3 = -\frac{q}{\pi}[\alpha - \sin\alpha]$$

where $\alpha = \theta_2 - \theta_1$. When the point M is on the surface, $\theta_2 = \theta_1$, $\alpha = 0$, and the principal stresses are zero.

In order to get a more refined/converged calculation, a linear, axisymmetric analysis was performed[27]. The finite element analysis (Figure 16) had sufficient high order, axisymmetric solid elements to assure convergence. While the calculated principal stresses were not zero, they were considerably reduced, as indicated in Figure 17 through Figure 20. The maximum tensile stress for this refined axisymmetric calculation, on the outer surface of the window, is 209 psi. This stress value is limited to the very inner and outer edges of the applied pressure annulus and is likely to be a numerical artifact. However, the tensile stress on the window surface is as high as 150 psi over a fairly extended region. While this doesn't agree with the analytical model, it may well be correct. Note that this stress is not much less than the stress due to bending under the atmospheric load. If the clamping pressure was increased (for example to get more compression in the o-ring for a lower leak rate), the resulting stress, due to clamping, could rival, or exceed, the stress due to the atmospheric load.
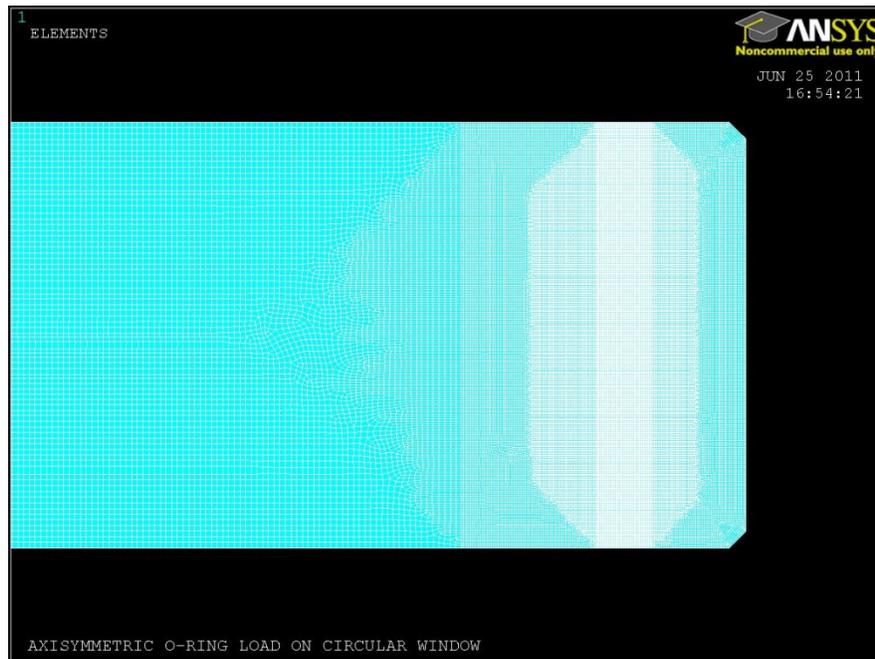
Figure 18 **Axisymmetric model of the response of the window to the clamping pressure.** (66,758 SOLID273, quadratic, axisymmetric elements)

---

[26] Adel Saada, <u>Elasticity Theory and Applications</u>, Krieger Pub. Co., 1993, section 14.9

[27] Using "Mechanical APDL (ANSYS 12.0)", also known as "classic ANSYS". ANSYS 12.0 WorkBench seemed to limit the number or size of axisymmetric elements.
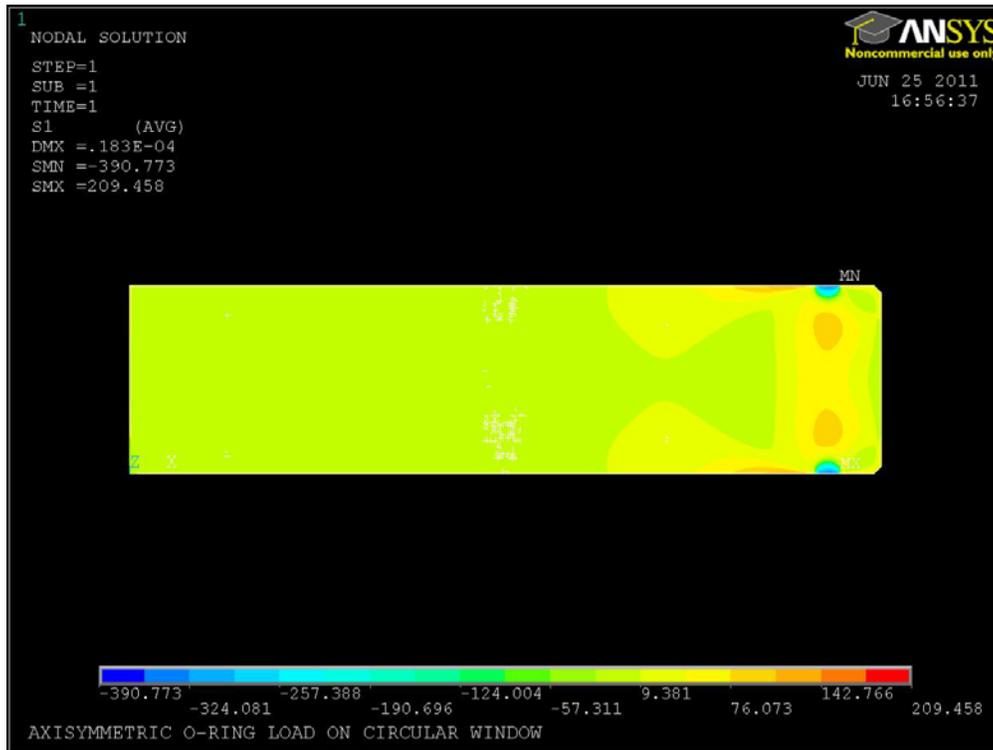
Figure 19   **Principal Stress, S1, for the axisymmetric model**
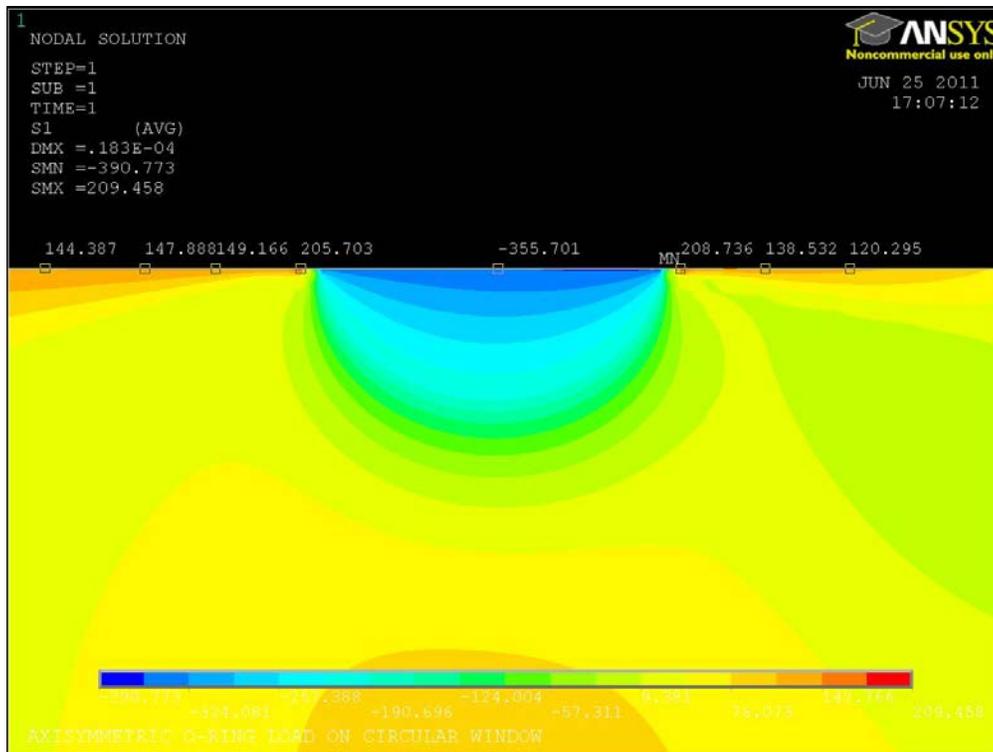
Figure 20   **Principal Stress, S1, for the axisymmetric model, in the region near the o-ring**
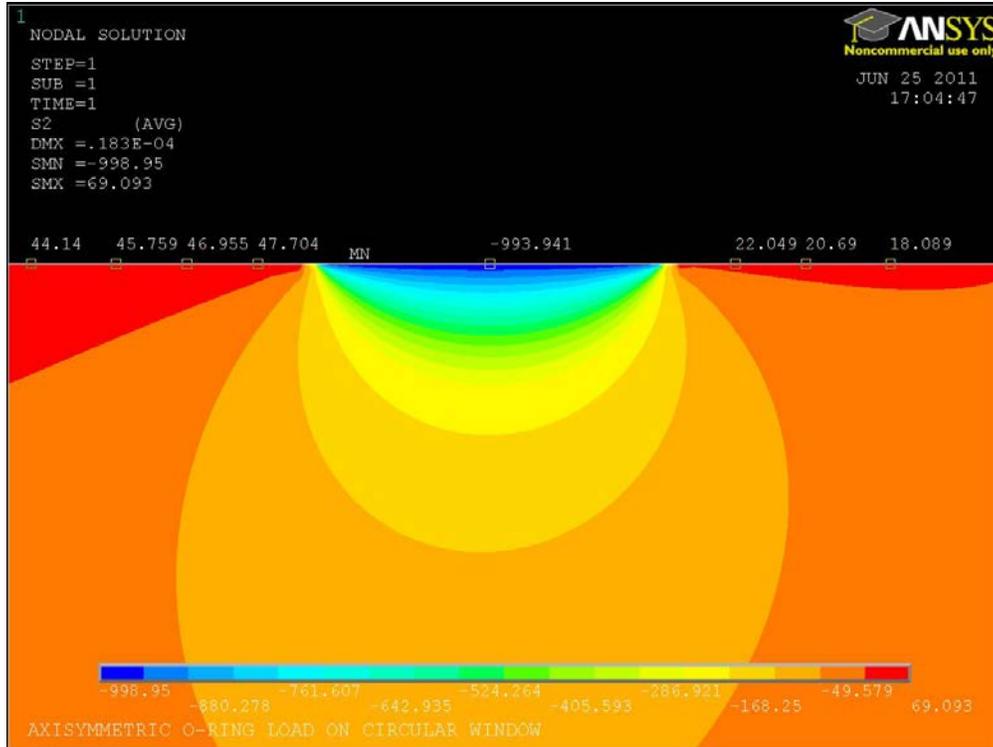
Figure 21   **Principal Stress, S2, for the axisymmetric model, in the region near the o-ring**
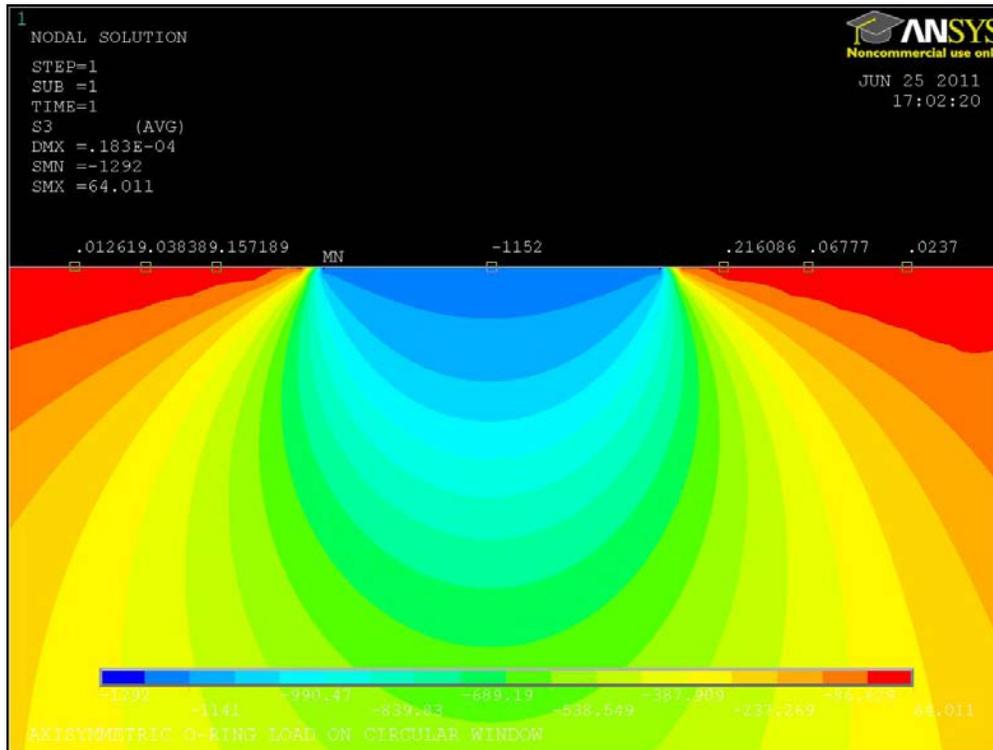
Figure 22   **Principal Stress, S3, for the axisymmetric model, in the region near the o-ring**

4.5 Design Factor of Safety and Proof Testing

In accordance with section 3.4.4 of the "Generic Requirements & Standards for Detector Subsystems"[28], the Factor of Safety (FS) for non-metallic, brittle structures should be a minimum of 3.0 for ultimate stress. This FS is to be used with a minimum ultimate strength value for the material. In addition section 3.4.4.1.1 calls for inert environment, proof testing with a factor of 1.2 (over the maximum in-service load) for all brittle, non-metallic materials on the vacuum envelope. For comparison:

- NASA guidance[29] for spaceflight hardware also requires that the structural integrity of glass components under pressure be verified by both analysis and testing. The analysis FS is 3.0 and the proof test factor is 2.0. Non-pressurized glass can be verified by either analysis with a FS = 5.0, or analysis with a FS = 3.0 and a proof test factor of 1.2. For protoflight hardware the proof testing duration is to be short and in an inert environment to minimize flaw growth.
- BNL guidance[30] employs a FS of 10 for glasses to establish an allowable design stress. This allowable design stress (680 psi) is approximately equal to the limit stress (740 psi) established in section 3.1. However here we apply a FS of 3.0 to this limit stress to arrive at an allowable design stress of only 247 psi. BNL does not stipulate a proof test requirement.
- The section on vacuum window safety[31] in Fermilab's E&SH Manual does not apply to optical windows. At least one Fermi Lab design references BNL's guidance for glass windows.

4.6 Stress Analysis Summary

The Margin of Safety (MS) is defined as

$$MS = \frac{\sigma_f}{FS\sigma_a} - 1$$

where σ_f is the failure, or limit, stress (defined in section 3.1), σ_a is the applied stress (calculated in sections 3.2 and 3.3) and FS = 3.0 is the design, or required, Factor of Safety (given in section 3.4). If the MS is positive the design is acceptable.

In the final design two, nominally identical, o-rings are used, so the moment due to the clamping/sealing forces is nominally zero. However, the opposing o-ring forces could create a moment due to the tolerance in the o-ring inner diameters. The moment due to the unbalanced clamping in section 3.3, was linearly scaled accordingly.

The stress analysis results are summarized in Table 4. The design is acceptable.

---

[28] D. Coyne, "Generic Requirements & Standards for Detector Subsystems", LIGO-E010613-v1

[29] "Structural Design and Test Factors of Safety for Spaceflight Hardware", NASA-STD-5001, 21 June 1996.

[30] "Guide for Glass and Plastic Window Design for Pressure Vessels", Brookhaven National Labs, 2.0/17606e011.doc, 6 Nov 2008.

[31] Fermilab ES&H Manual, "Vacuum Window Safety", 5033.1, 04/2010

Table 6　　　Summary of Margins of Safety for each loading condition

Loading Condition	FEA Max Tensile Stress (psi)	Margin of Safety (MS)	Comments
Atmospheric pressure	213	+0.16	
Clamping Load: @ window center	94	+1.6	moment due to o-ring I.D. tolerance (±.035")
Clamping Load: near clamp	209	+0.18	For maximum force corresponding to a Shore A hardness of 80. The maximum stress may be a numerical artifact; could be only 150 psi

5 Proof Test

The "LIGO Generic Requirements & Standards for Detector Subsystems" (section 3.4.4.1.1) calls for inert environment, proof testing with a factor of 1.2 (over the maximum in-service load) for all brittle, non-metallic materials on the vacuum envelope. A better approach is to proof test in the intended environment at a proof stress which guarantees the desired minimum lifetime[14,32]. The minimum lifetime after proof testing is given by:

$$t_{min} = B\sigma_p^{N-2}\sigma_a^{-N}$$

where σ_p is the proof stress, σ_a is the applied, or service, stress and N and B are fracture mechanics material parameters defined in section 4.1. The applied/service stress is the result of 1 atmosphere of differential pressure load. A proof test would impose a higher differential pressure in order to get the same stress field response except at higher amplitude. Due to the linear elastic response of the window, the proof stress can be expressed as a multiple of the applied/service stress:

$$\sigma_p = x\sigma_a$$

where x is the number of atmospheres of load to be used in the proof test and σ_a is 213 psi [1.47 MPa]. With a required t_{min} of 20 years, the proof test pressure is 2.11 atmospheres.

However this proof pressure is high enough that the gap between the glass and the viewport flange will close and cause contact between the glass and metal. An atmosphere of pressure differential over the o-ring ID results in a load of 19.7 lbs/in of o-ring. From the o-ring compression chart (Figure 12), we see that to create this differential load requires a difference in compression ratios, between the two o-rings, of ~20%. For the nominal o-ring diameter (.139"), this corresponds to one o-ring compressing .014" more and one compressing .014" less. This leaves barely sufficient gap clearance in the nominal, balanced o-ring case (.004" gap). At a proof test load of 2.11 atm, the glass would press against the metal. As a consequence either (a) a protective thin shim of soft material is placed between the glass and the metal (e.g. kapton), or (b) the window is proof tested separately from the viewport assembly and care is taken not to compromise the glass surface is subsequent handling and assembly.

---

[32] J. Ritter, D. Coyne, K. Jakus, "Failure Probability at the Predicted Minimum Lifetime After Proof Testing", Journal of the American Ceramic Society, Vol. 61, No.5-6, pp. 213-216